

## Corrosion of pipe steels under alternating currents

Ajit Kumar Thakur<sup>1</sup>, Adarsh Kumar Arya<sup>1\*</sup>, Pushpa Sharma<sup>2</sup>

<sup>1</sup> Department of Chemical Engineering, UPES, Dehradun, INDIA

<sup>2</sup> Department of Petroleum and Energy Studies, UPES, Dehradun, INDIA

\*E-mail: [akarya@ddn.upes.ac.in](mailto:akarya@ddn.upes.ac.in)

Received: 5 August 2021 / Accepted: 30 September 2021 / Published: 10 November 2021

---

The present paper aims to analyze and compare AC interference on pipeline steel grades in soil simulating solutions. DC current density ( $J_{DC}$ ) and protection potential (PP) are measured to determine AC interference. The study presents the corrosion resistance of several grades of steel. The paper describes experimental studies involving potentiostatic and galvanostatic measurements. The experimental arrangement has been set up for AC and DC couplings to measure DC current density ( $J_{DC}$ ), protection potential (PP), and AC current density ( $J_{AC}$ ). The paper presents findings on the AC corrosion behavior of different pipeline steels based on variation in AC current density. The study shows the comparative performance of varying pipe steels. Experimental studies have been conducted on pipe steel in soil simulating solutions under controlled conditions using a specially designed experimental setup. Special care in the experimental setup prevents errors in measurements due to IR drop. The behavior in the field may be influenced by other factors also. The results may be helpful to the pipeline industry in making informed selections of pipe steels subjected to AC interference.

---

**Keywords:** Cathodic protection, Pipeline corrosion, X grade pipeline, Protection Potential, Alternating current density

### 1. INTRODUCTION

The need for transporting massive amounts of oil and gas has prompted an interest in developing an efficient method of transportation. Pipelines have been considered a sound way to transport oil and gas since the beginning of modern civilization. [1-2; 38-39]. The pipelines ensure the safe and environmentally responsible transportation of hazardous substances. Experts recommend monitoring the pipeline networks continuously to ensure their integrity. The health of the pipeline system affects people's health and the environment. An accident involving a pipeline would have disastrous consequences for the ecosystem.

Corrosion monitoring and protection is a critical component of pipeline integrity maintenance. Corrosion [3] related failures are the leading cause of pipeline integrity failures (65 percent in oil and 34

percent in gas service). The application of an appropriate coating to the steel pipeline serves as the principal corrosion prevention system. A secondary corrosion prevention system typically contains a cathodic protection (CP) system to ensure the pipeline system's long-term integrity. The CP system improves the effectiveness of primary coatings in preventing corrosion [4, 5]. Cathodic protection systems provide direct current circulation between the cathode (pipeline) and anode (ground) via electrolytic processes, including oxidation and reduction, preventing pipe corrosion in the soil. CP system polarizes and forms a passive film on the surface of pipe steel. The commonly accepted conditions [6, 7] for pipeline corrosion prevention include polarising pipelines in the negative direction by more than (-) 850 mV. Polarisation of more than (-) 850 mV is insufficient to defend against corrosion.

Voltage transfer may occur from power lines to pipelines when they are situated close to each other. Such voltages can increase exponentially in the presence of a power line fault condition. When a pipeline is adjacent to a high-voltage transmission line, it may carry voltage. Other than the high risk of injury to service workers, it may also reduce the steel quality in the pipe. Alternating current interference renders the parameters listed here inadequate for corrosion protection.

Experiments [8] on carbon steel pipe samples exposed to varying AC current densities under CP demonstrated that the (-) 850 mV threshold is inadequate. With induced AC, the negative polarization potential of (-) 850 mV may not be sufficient to defend against corrosion [9]. The application of the coating on a prolonged basis is harmful if it is above (-) 1200 mV in the negative direction.

For pipeline networks, cathodic protection techniques consider the pipe-to-soil potential (PSP), the ratio of AC/DC current density, and the AC current density ( $J_{AC}$ ). AC corrosion factors such as the AC/DC current density ratio, the AC current density ( $J_{AC}$ ), and the alternating voltage (AV) are crucial. Corrosion is possible at AC current densities of between 30 and 100 A/m<sup>2</sup>, and damage from AC corrosion is likely at densities of more than 100 A/m<sup>2</sup> [24]. Conventional CP procedures are unsuccessful at protecting pipelines from corrosion caused by AC interference [10-12]. A touch potential of 15 V or greater caused by induced AC [13] poses a severe concern for worker safety.

Electromagnetic induction causes interference with pipelines due to closeness to transmission lines, creating resistive, capacitive, and inductive coupling [14, 15]. Corrosion problems linked with AC interference have developed dramatically in proximity to buried pipelines [16, 17]. Different experiments and studies have attempted to quantify and assess AC interference [18-23].

In the presence of AC, avoid excessive protection should since it results in severe corrosion [8]. A 2020 study [25] shows that the effect of variable AC corrosion with increasing interference time is similar to that of steady-state AC corrosion. Increased AC/DC current density suggests an increased risk of decay. A reduced current density ratio implies a lower probability of corrosion but does not assure corrosion prevention. AC moderation techniques, such as pipeline grounding, are required to reduce the amplitude of coating stress voltage and hence the likelihood of AC corrosion [26, 27]. Algorithms for assessing induced current and voltage are increasingly being explored [27]. The passive film is mainly unaffected by lower AC densities, resulting in minor polarization potential changes. Pipeline steel is subjected to extensive localized corrosion attack at higher AC densities, whereas uniform corrosion occurs at lower AC densities [28, 29]. Corrosion is also affected by the characteristics of coating pores [30]. The shift in potential for polarisation caused by AC is due to the increased corrosion current caused

by passive film breakdown [5]. AC forms a thin passive film and increases the chances of it collapsing [31–33].

The applied coating on the metal surface and soil resistivity influence the demand of CP current density (Table 1) to achieve cathodic protection of bare metal surface within a short span.

The present study aims to ascertain how alternating current interference affects the steel in underground pipelines. Additional mitigating procedures are necessary to mitigate the effect of AC interference on pipelines. AC corrosion tests under similar circumstances are essential to evaluate the relative performance of different pipe steel types. This study bridges the gap by evaluating and assessing the corrosion resistance of many other pipeline plates of steel. Investigations include performing potentiostatic and galvanostatic tests in soil mimicking solutions to assess pipe steels' resistance to AC corrosion.

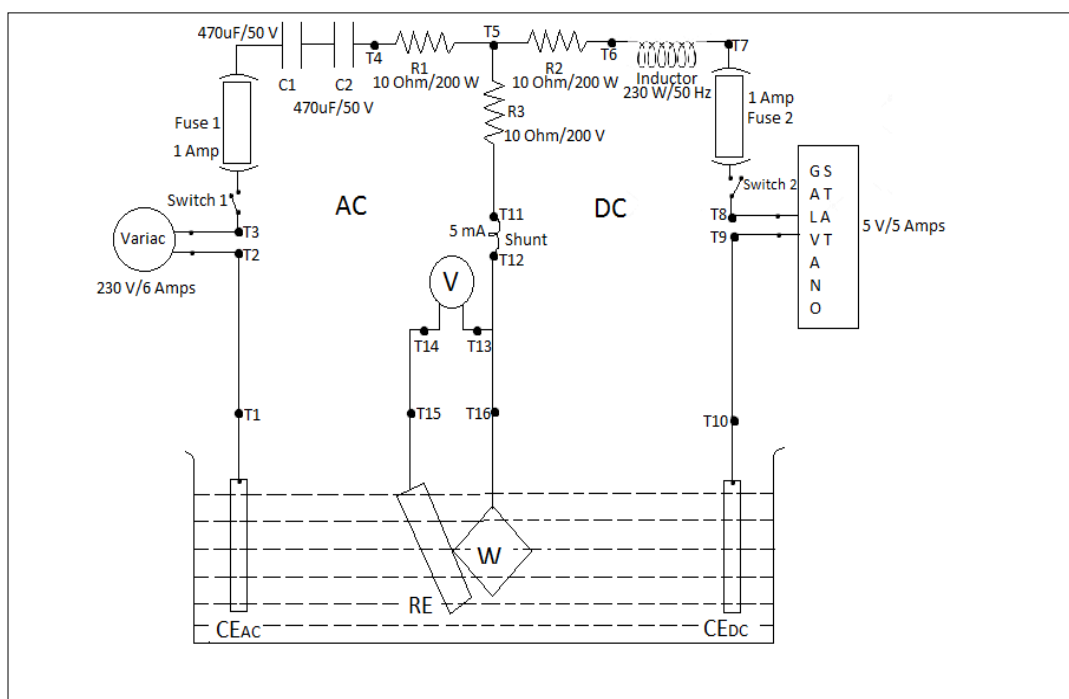


**Figure 1.** Experimental Circuitry with AC and DC circuits coupled using Capacitors and Inductors. Shunts enable the measurement of DC current density ( $J_{DC}$ ) and AC current density ( $J_{AC}$ ). The potential of the specimen is measured using the Cu-CuSO<sub>4</sub> Reference electrode.

## 2. EXPERIMENTAL

The present section details the methodology used to ascertain the impact of alternating current on pipe steel.

### 2.1. AC and DC Electrical Circuits

The specially designed suitably coupled AC and DC circuits (Figure 1) prevented interference between the two circuits. The coupling leveraged the fundamental features of inductors and capacitors.

In a direct current circuit, an inductor inhibits the circulation of alternating current, while a capacitor blocks the circulation of direct current in an alternating current circuit [34]. Through the pipe specimen, the variable autotransformer provided the necessary alternating current. A galvanostat injected the required DC into the pipe specimen. While AC flow provided the required current for AC interference, DC flow maintained the pipe specimen's corrosion-free state. Shunts measured current flow, and counter electrodes completed necessary circuits. The specimen's potential was determined using the Cu-CuSo<sub>4</sub> reference electrode.

## 2.2. Preparation of Steel Specimen and Solution for Simulating Soil

The wide use of pipe grades (API 5L) in oil and gas pipelines is due to their appropriateness for sour service, prolonged duration of service, and opposition to crack spreading. API 5L steels are resistant to corrosion and have a high tensile and yield strength. These pipes' composition and microstructure can vary significantly depending on the carbon, manganese, sulfur, and phosphorous concentration limits. Steel specimen of the respective grade measured 6 mm in thickness and 100 mm in diameter.

Each specimen, after washing, is inserted into a cylindrical PVC tube with an internal diameter of 10 mm with a length of 40 mm. Welding a copper cable (6 mm<sup>2</sup>) to one of the specimen's faces provides an electrical connection. A bare surface is available on the opposite facet of the sample. The PVC tube is then filled with epoxy to provide an airtight seal and prevent moisture ingress. The simulating soil solution contained 200 mg chlorides and 500 mg sulfates per liter of clean water at room temperature. The test solution used purified water and analytic-grade reagents. Tests performed involving novel solution each time and the previous solution discarded after the test. The soil solution is a popular NS4 solution that is close to neutral.

## 2.3. Measuring the protection potential (PP) with different AC current density ( $J_{AC}$ )

Each specimen is dipped in a solution simulating soil to measure the protection potential at different AC densities. It is essential to examine the alternating current's effect on the protection potential by varying the DC with a galvanostat. Different alternating current densities in steps interfere with the DC current densities and monitor the protection potential. After applying a DC current density ( $J_{DC}$ ) of 0.01 A/m<sup>2</sup> for 24 hours without AC, measured the protection potential. Subsequently, administered 30 minutes of alternating current density ( $J_{AC}$ ) in steps of 10, 30, 50, 100, and 200 A/m<sup>2</sup>. For each stage, measured the sample potential at an interval of 5 minutes.

## 2.4. Measurement of DC current density ( $J_{DC}$ )

Alternating current is deployed in potentiostatic tests to measure DC current density ( $J_{DC}$ ) variation by changing the protection potential in steps at various AC current densities. Conducted the potentiostatic test to determine the effect of alternating current on the DC current density ( $J_{DC}$ ) by applying a protection potential of (-) 0.850 V for 24 hours without AC. Subsequently, administered 30 minutes of alternating current density ( $J_{AC}$ ) in 10, 30, 50, 100, and 200 A/m<sup>2</sup> steps. For each stage, measured the DC current density ( $J_{DC}$ ) every 5 minutes.

**Table 1.** Soil resistivity, Coating Type, and Design current density

S. No.	Soil resistivity ( $\Omega\text{m}$ )	Design current density ( $\mu\text{A}/\text{m}^2$ )		
		Fusion Bonded Epoxy coating	Three Layer Polyethylene coating	Coal tar Enamel coating
1	<10	70	50	150
2	10-100	50	25	125
3	>100	25	15	75

### 3. RESULTS AND DISCUSSION

#### 3.1. AC Interference Analysis

##### 3.1.1. X46 Steel

The DC current density ( $J_{DC}$ ) increased from  $0.020 \text{ A}/\text{m}^2$  to  $0.054 \text{ A}/\text{m}^2$ , at a potential of (-) 850 mV, with a variation in AC current density ( $J_{AC}$ ) in steps from  $10 \text{ A}/\text{m}^2$  to  $200 \text{ A}/\text{m}^2$ , indicating an increase (Figure 2) of 179% in DC current density ( $J_{DC}$ ).

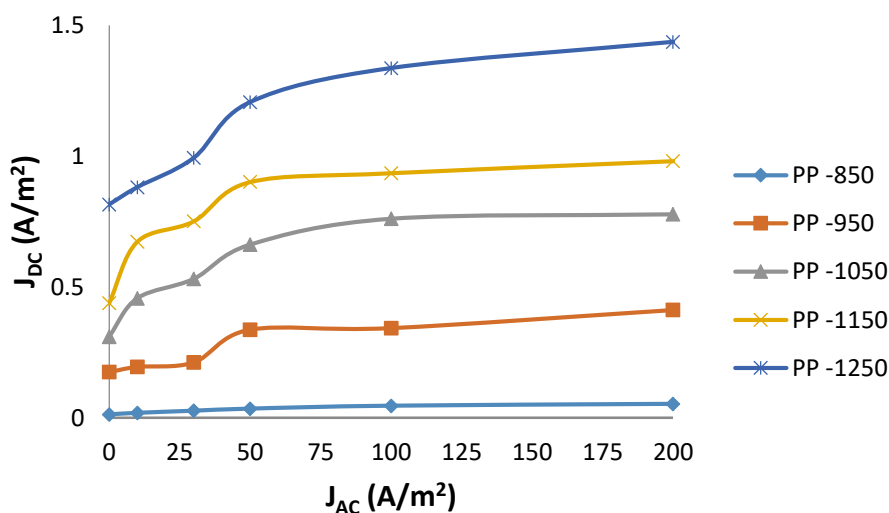


**Figure 2.** DC current density ( $J_{DC}$ ) variation with AC current density ( $J_{AC}$ ) at protection potentials ((-) 850, (-) 950, (-)1050, (-) 1150, and (-) 1250 mV) for X46 steel in soil simulating solution.

With a potential of (-) 950 mV, the protection density increased from  $0.196 \text{ A}/\text{m}^2$  to  $0.413 \text{ A}/\text{m}^2$  with variation in AC current density ( $J_{AC}$ ) from  $10 \text{ A}/\text{m}^2$  to  $200 \text{ A}/\text{m}^2$ , indicating an increase of 111% in DC current density ( $J_{DC}$ ). The percentage change in DC current density ( $J_{DC}$ ) is low for protection potential variation from (-) 1050 mV to (-) 1250 mV. The results align with earlier investigations [35] which concluded that the CP protection levels influence AC interference, and DC current density ( $J_{DC}$ )

higher than 5 A/m<sup>2</sup> may result in AC corrosion. For X46 steel, specimens remain protected at a DC current density ( $J_{DC}$ ) of 0.1 A/m<sup>2</sup> without AC interference at a protection potential of (-) 1069 mV.

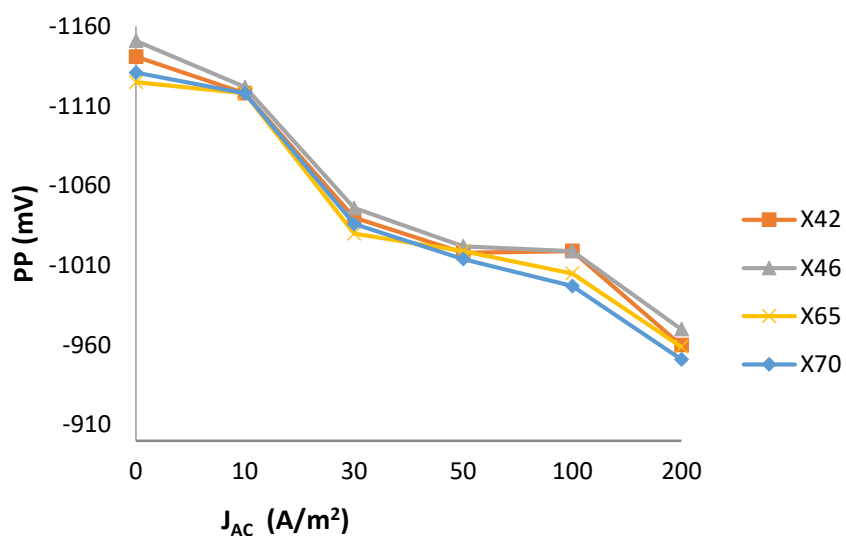


**Figure 3.** Protection potential (PP) with AC current density ( $J_{AC}$ ) at a DC current density ( $J_{DC}$ ) of 0.3 A/m<sup>2</sup> for X42, X46, X65, and X70 steels in soil simulating solution.

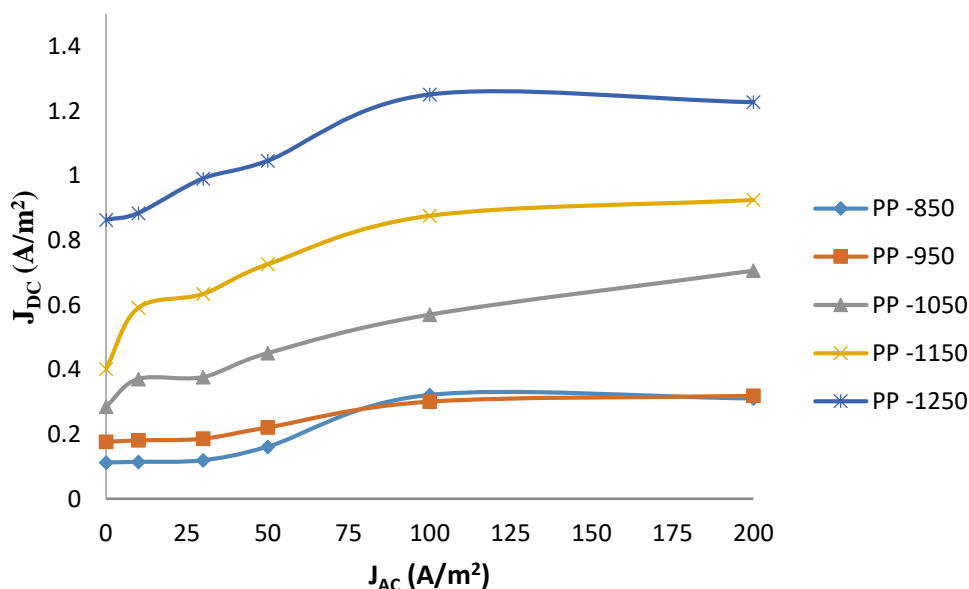


**Figure 4.** DC current density ( $J_{DC}$ ) variation with AC current density ( $J_{AC}$ ) at protection potentials ((-) 850, (-) 950, (-)1050, (-) 1150, and (-) 1250 mV) for X42 steel in soil simulating solution.

The increase in DC current density ( $J_{DC}$ ) from 0.1 A/m<sup>2</sup> to 10 A/m<sup>2</sup> made the potential more hostile, improving corrosion prevention. At a DC current density ( $J_{DC}$ ) of 0.3 A/m<sup>2</sup>, the protection potential of X46 steel samples varied from (-) 1151 mV to (-) 970 mV, with an AC current density ( $J_{AC}$ ) change from 0 A/m<sup>2</sup> to 200 A/m<sup>2</sup> (Figure 3). Published research [36] has observed the AC corrosion rate at an AC current density of 10 A/m<sup>2</sup> to be twice the corrosion rate without AC. It is evident here that the

AC corrosion rate at a particular AC current density may vary depending upon the level of steel polarization. The observation is in close agreement with a published study that concluded that the direction of potential shifting depends upon applied CP [33]. At the protection potential (PP) of (-) 1150 mV, the DC current density ( $J_{DC}$ ) is almost constant for X46 pipe, with variation in AC current density ( $J_{AC}$ ) from 50 A/m<sup>2</sup> to 100 A/m<sup>2</sup>, indicating better corrosion performance of X46 steel to other steels. High pitting corrosion due to specific AC current density is likely at higher DC current densities in line with available literature [11, 12].

### 3.1.2. X42, X65, and X70 Steel

For X42 steel, the DC current density ( $J_{DC}$ ) increased (Figure 4) from 0.114 A/m<sup>2</sup> to 0.31 A/m<sup>2</sup> at a protection potential of (-) 850 mV, with a change in AC current density ( $J_{AC}$ ) in steps from 10 A/m<sup>2</sup> to 200 A/m<sup>2</sup>, indicating a 176% jump in DC current density ( $J_{DC}$ ).

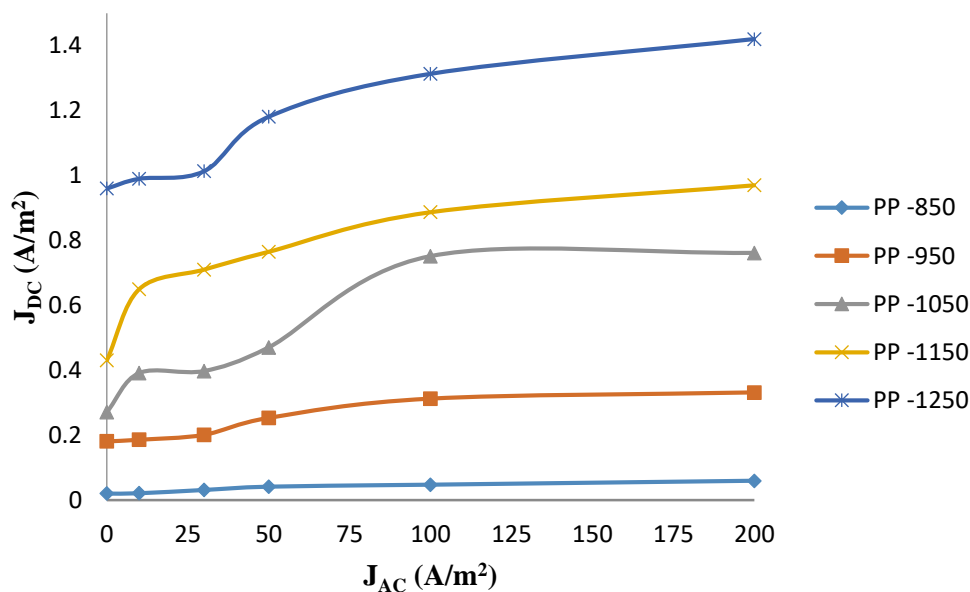


**Figure 5.** DC current density ( $J_{DC}$ ) variation with AC current density ( $J_{AC}$ ) at protection potentials ((-) 850, (-) 950, (-)1050, (-) 1150, and (-) 1250 mV) for X65 steel in soil simulating solution.

With a potential of (-) 850 mV for X65 steel, the DC current density ( $J_{DC}$ ) changed from 0.022 A/m<sup>2</sup> to 0.060 A/m<sup>2</sup> with a variation in AC current density ( $J_{AC}$ ) from 10 A/m<sup>2</sup> to 200 A/m<sup>2</sup>, indicating a 181% jump (Figure 5) in DC current density ( $J_{DC}$ ). For X70, observed a 167% jump in DC current density ( $J_{DC}$ ). The different percentage increases are attributable to the pipe steel's unique microcrystalline structure. The Gibbs free energy change, resulting in a negative shift in corrosion potential, explains the tendency of enhanced corrosion [29] and agrees well with the results obtained.

For X65 steel, samples are protected at a DC current density ( $J_{DC}$ ) of 0.1 A/m<sup>2</sup> with a potential of (-) 1061 mV with no AC. The protection potential shifted negatively with the increase in DC current density ( $J_{DC}$ ), indicating better corrosion prevention. With a DC current density ( $J_{DC}$ ) beyond 0.5 A/m<sup>2</sup>,

the protection potential exceeds (-) 1200 mV. Overprotection conditions after some time may lead to coating damage. At a DC current density ( $J_{DC}$ ) of  $1 \text{ A/m}^2$ , the protection potential of X65 steel samples changed from (-) 1241 mV to (-) 1065 mV, with a variation in AC current density ( $J_{AC}$ ) from  $0 \text{ A/m}^2$  to  $200 \text{ A/m}^2$ . The severe damage to passive film at AC current densities ranging from 50 to  $200 \text{ A/m}^2$  leading to enhanced corrosion (Figure 6). Up to an AC current density ( $J_{AC}$ ) of  $10 \text{ A/m}^2$ , X65 exhibits comparable corrosion resistance. The passive film quickly deteriorates, at higher AC current densities, allowing the protection potential to shift positively.

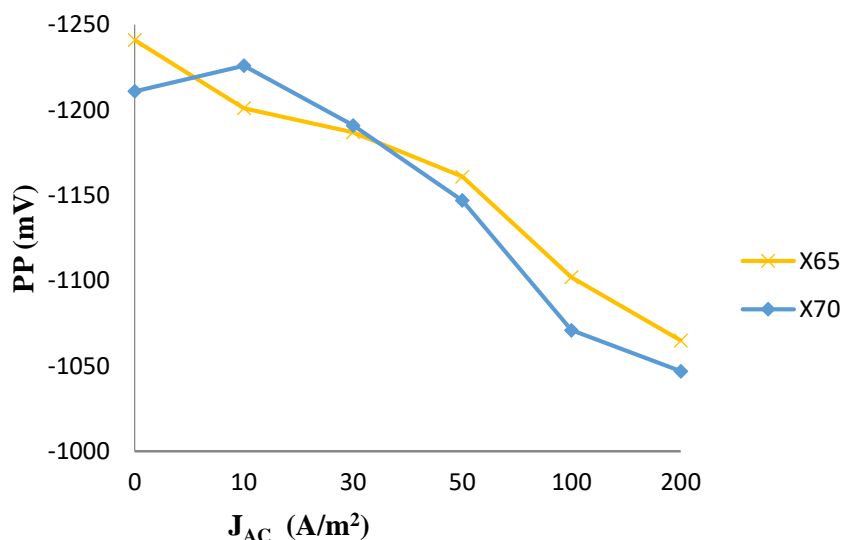


**Figure 6.** Protection potential (PP) of X65 and X70 steels with change in AC current density ( $J_{AC}$ ), at a DC current density ( $J_{DC}$ ) of  $1 \text{ A/m}^2$  in soil simulating solution

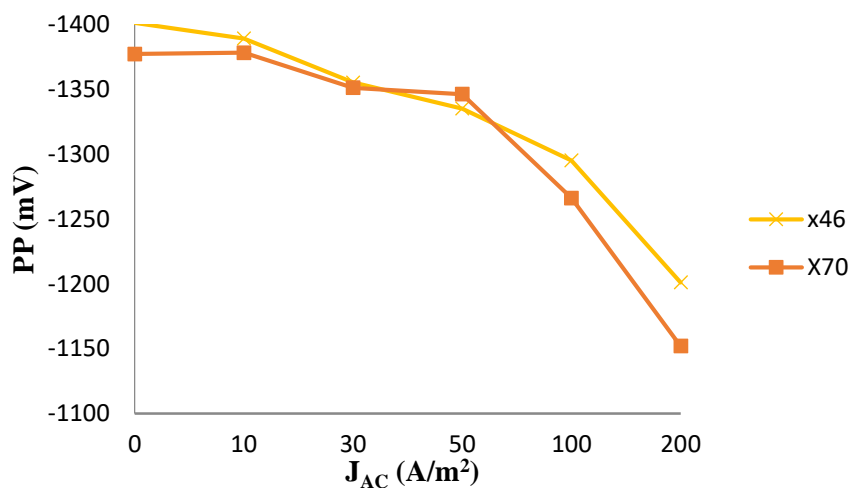


**Figure 7.** Protection potential (PP) of X46 and X70 steels with AC current density ( $J_{AC}$ ) at a DC current density ( $J_{DC}$ ) of  $10 \text{ A/m}^2$  in soil simulating solution.



At a DC current density ( $J_{DC}$ ) of 0.3 A/m<sup>2</sup>, the protection potential of X70 grade steel samples shifted to (-) 959 mV from (-) 1125 mV with variation in AC current density ( $J_{AC}$ ) in steps from 0 A/m<sup>2</sup> to 200 A/m<sup>2</sup>. AC corrosion occurs at lower AC densities with a positive potential change in the X65 and X70 samples. The protection potential for the X70 pipe shifted to (-) 839 mV from (-) 1061 mV due to a change in AC current densities (Figure 7). With an AC current density ( $J_{AC}$ ) of 200 A/m<sup>2</sup> at a DC current density ( $J_{DC}$ ) of 0.1 A/m<sup>2</sup>, X70 steel could not satisfy the (-) 850 mV protection criterion, which may result in accelerated corrosion. Protection current cannot prevent corrosion at larger AC densities, which agrees with the available publication [37].

#### 4. CONCLUSION

The DC protection current density ( $J_{DC}$ ) increases initially with a variation in AC current density ( $J_{AC}$ ) from 0 A/m<sup>2</sup> to 30 A/m<sup>2</sup> for all pipe steels. The passive film on the metal surface is intact at lesser AC current densities, thereby resisting AC corrosion. However, observed no significant change in DC current density with AC current densities from 50 A/m<sup>2</sup> to 200 A/m<sup>2</sup>. The inactive film at high AC densities is increasingly unstable, decreasing thickness and significant damage, leading to enhanced corrosion. For the X46 pipeline, the substantial percentage rise in DC current density illustrates the CP system's ability to provide adequate cathodic protection at lower potentials. However, at protection potentials more negative than (-) 1200 mV, overprotection may eventually lead to severe coating failure.

For X42 and X46 steels, protection potential shifted positively with variation in AC current density. Experimental data indicates that steel of the X42 and X46 grades exhibit a similar response to AC interference. The higher positive potential shift for X65 and X70 grades steels with increased AC current density to 100 A/m<sup>2</sup> indicates higher susceptibility to corrosion at a DC current density ( $J_{DC}$ ) of 1 A/m<sup>2</sup>. The X65 and X70 steels are likely to corrode more rapidly when exposed to AC interference, which could be because of the differences in the microstructure and morphology of steel. Factors like soil resistivity and pH may also affect the corrosion prevention response.

Corrosion protection of the steel sample is due to thick passive film on the sample surface. With no AC, pipe samples remain protected at a DC current density ( $J_{DC}$ ) of 0.1 A/m<sup>2</sup>. However, with the increasing density of protective currents, protection potential has become more negative. The steel of all grades shows a DC current density ( $J_{DC}$ ) of 1 A/m<sup>2</sup>, a protection potential higher than (-) 1200 mV in the negative direction, which may severely damage the coating over time and lead to localized corrosion.

Pipeline engineers to address AC corrosion behavior while selecting the suitable pipe steel for the necessary application. Additional modeling/optimization studies are required to determine appropriate measures for the mitigation of AC corrosion. Additionally, design mitigation methodologies to minimize deterioration due to AC interference.

#### ACKNOWLEDGMENT

Any specific public, commercial, or not-for-profit funding agencies did not support this research.

## NOMENCLATURE:

<b>AC</b>	Alternating Current
<b>DC</b>	Direct Current
<b>API</b>	American Petroleum Institute
<b>CP</b>	Cathodic Protection
<b>pH</b>	Power of Hydrogen, a measure of acidity or alkalinity of a solution

## References

1. A. K. Arya, and S. Honwad, *J. Pet. Explor. Prod. Technol.*, 8 (2018) 1389.
2. A. K. Arya, and S. Honwad, *J. Pipeline Syst. Eng. Pract.*, 1 (2016) 04015008.
3. Z. M. Hossein, S. Deif, and M. Daneshmand, *Sens. Actuators, A*, 261 (2017) 24.
4. D. H. Kroon, and M. Urbas, *Mater. Perform.*, 33 (1994) 26.
5. S. Goidanich, L. Lazzari, and M. Ormellese, *Corros. Sci.*, 52 (2010) 491.
6. D. Z. Tang, Y. X. Du, M. X. Lu, Y. Liang, Z. T. Jiang, and L. Dong, *Mater. Corros.*, 12 (2015) 1467.
7. M. Büchler, *Corrosion*, 76 (2020) 451.
8. A. Brenna, L. Luciano, P. Mariapia, and M. Ormellese, *Metall. Ital.*, 6 (2014) 29.
9. D. Kuang, and Y. F. Cheng, *Corros. Eng., Sci. Technol.*, 52 (2017) 22.
10. Y. B. Guo, C. Liu, D. G. Wang, and S. H. Liu, *Pet. Sci.*, 12 (2015) 316.
11. S. B. Lalvani, and X. A. Lin, *Corros. Sci.*, 36 (1994) 1039.
12. S. B. Lalvani, and G. Zhang, *Corros. Sci.*, 37 (1995) 1567.
13. J. Mystkowska, K. Niemirowicz-Laskowska, D. Lysik, G. Tokajuk, J. R. Dabrowski, and R. Bucki, *Int. J. Mol. Sci.*, 19 (2018) 743.
14. M. Zhu, C. Du, X. Li, Z. Liu, S. Wang, J. Li., and D. Zhang, *Electrochim. Acta*, 117 (2014) 351.
15. B. P. Kumleh, H. V. Mohammad, and S. P. Kumleh, *IFAC Proceedings Volumes* 36 (2003) 1151.
16. A. K. Thakur, A. K. Arya, and P. Sharma, *Corros. Rev.* 38 (2020) 463.
17. I. S. Cole, and D. Marney, *Corros. Sci.*, 56 (2012) 5.
18. M. Zhu, Y. Yuan, S. Yin, and S. Guo, *Int. J. Electrochem. Sci.*, 13 (2018) 10669.
19. D. Kuang, and Y. F. Cheng, *Corrosion*, 71 (2015) 267.
20. M. A. Azam, S. Sukarti, and M. Ziami, *Eng. Fail. Anal.*, 115 (2020) 104654.
21. D. Kuang, and Y. F. Cheng, *Corros. Sci.* 85 (2014) 304.
22. D. Kuang, and Y. F. Cheng, *Corros. Sci.* 99 (2015) 249.
23. F. E. Kulman, *Corrosion*, 17 (1961) 34.
24. S. Goidanich, L. Luciano and M. Ormellese, *Corros. Sci.*, 52 (2010) 916.
25. L. Chen, D. Yanxia, Y. Liang and L. Jianjun, *Corros. Eng., Sci. Technol.*, 56 (2021) 219.
26. C. Wen, J. Li, S. Wang, and Y. Yang, *J. Nat. Gas Sci. Eng.*, 27 (2015) 1555.
27. G. Lucca, *IET Sci., Meas. Technol.*, 15 (2021) 25.
28. A. Q. Fu, and Y. F. Cheng, *Corros. Sci.* 52 (2010) 612.
29. Y. Li, C. Xu, R. H. Zhang, Q. Liu, X. H. Wang, and Y. C. Chen, *Int. J. Electrochem. Sci.*, 12 (2017) 1829.
30. Z. Jiang, Y. du, M. Lu, Y. Zhang, D. Tang, and L. Dong, *Corros. Sci.*, 81 (2014) 1.
31. M. Zhu, and C. W. Du, *J. Mater. Eng. Perform.*, 26 (2017) 221.
32. M. Zhu, J. L. Yang, Y. B. Chen, Y. F. Yuan, and S. Y. Guo., *Mater. Eng. Perform.*, 29 (2020) 423.

33. H. Wang, C. Du, Z. Liu, L. Wang, and D. Ding, *Materials*, 10 (2017) 851.
34. A. K. Thakur, A. K. Arya, and P. Sharma. *Mater. Today. Proc.*, (2021) 1.
35. L. Chen, Y. Du, Y. Liang, and J. Li, *Corros. Eng., Sci. Technol.*, 56 (2021) 219.
36. D. K. Kim, T. H. Ha, Y. C. Ha, J. H. Bae, H. G. Lee, D. Gopi, and J. D. Scantlebury, *Corros. Eng., Sci. Technol.*, 39 (2004) 117.
37. H. Qin, Y. Du, M. Lu, X. Sun, and Y. Zhang, *Mater. Corros.*, 71 (2020) 1856.
38. A.K. Arya, and S. Honwad, *Chem. Prod. Process Model.*, 13 (2018) 1.
39. A. K. Arya, *J. Pet. Explor. Prod. Technol.*, (2021) 1.

© 2021 The Authors. Published by ESG ([www.electrochemsci.org](http://www.electrochemsci.org)). This article is an open access article distributed under the terms and conditions of the Creative Commons Attribution license (<http://creativecommons.org/licenses/by/4.0/>).